Probing cellular events, one quantum dot at a time

Fabien Pinaud[1,2], Samuel Clarke[1,2], Assa Sittner[1] & Maxime Dahan[1]

Monitoring the behavior of single molecules in living cells is a powerful approach to investigate the details of cellular processes. Owing to their optical, chemical and biofunctional properties, semiconductor quantum dot (QD) probes promise to be tools of choice in this endeavor. Here we review recent advances that allow ever more controlled experiments at the single-nanoparticle level in live cells. Several examples, related to membrane dynamics, cell signaling or intracellular transport, illustrate how single QD tracking can be readily used to decipher complex biological processes and address key concepts that underlie cellular organization and dynamics.

Recent reports have emphasized the tremendous potential of single quantum dot (QD) imaging techniques in cell biology. In these experiments, the motion of single molecules, labeled with fluorescent QDs, is monitored in live cells over time scales from milliseconds to hours. Individual trajectories of the molecules can be determined with nanometer accuracy, a scale similar to that of molecular interactions. Therefore, single-QD tracking (SQT) constitutes an exquisitely sensitive tool to explore how molecules are dynamically orchestrated in cells to form assemblies that ensure cellular structures and functions.

SQT techniques build on concepts introduced by single-particle tracking methods in the late 1980s[1]. In single-particle tracking measurements, micrometer-sized latex beads or 40–100 nm gold nanoparticles, detected by interference contrast microscopy, are used to follow single molecules in live cells. This approach recently was extended to track single dyes or fluorescent proteins in cells[2]. Over the years, tracking techniques and the development of various targeting, processing and modeling methods have been instrumental to study, among others, the heterogeneous and dynamic organization of the plasma membrane. Nevertheless, the widespread use of these techniques has remained hindered by several experimental factors, including the large probe size, the limiting optical properties of the probes or the difficulties in implementing multiparametric imaging.

The recent advent of functional colloidal QDs largely expands the range of applications for tracking measurements. Originally QD probes were promoted for their signature optical spectrum, namely a wide absorbance and narrow, symmetric emission with size-dependent peak position. These features result in a large effective Stokes' shift and simplify the technical requirements for multicolor detection[3]. Later, it was shown that they are also good labels for single-molecule experiments in live cells[4]. Their moderate size (10–40 nm), bright fluorescence and excellent resistance to photobleaching, make QDs a favorable compromise between large beads and small yet poorly photostable dyes to achieve high-sensitivity imaging assays in noninvasive conditions. Moreover, the availability of many surface functionalization schemes provides strategies for efficient QD targeting. Altogether, QDs allow multiparametric single-molecule experiments that could have hardly been envisioned with prior methods.

Here we review the principles and methods behind SQT experiments and present recent progress in QD chemistry, functionalization and image processing that solve many issues associated with the tracking of single nanoparticles. Several examples show how experiments addressing membrane dynamics, internalization pathways or intracellular transport have already benefited from the high sensitivity of SQT

[1]Laboratoire Kastler Brossel, Centre National de la Recherche Scientifique Unité de recherche 8552, Physics and Biology Department, Ecole normale supérieure, Université Pierre et Marie Curie, Paris 6, Paris, France. [2]These authors contributed equally to this work. Correspondence should be addressed to M.D. (maxime.dahan@lkb.ens.fr).

PUBLISHED ONLINE 30 MARCH 2010; DOI:10.1038/NMETH.1444

assays. Finally, we discuss challenges that still need to be addressed to make SQT a standard method in cell biology.

A single-molecule approach to cell imaging

Over the past decade, progress in single-molecule research has contributed many practical and conceptual tools to visualize individual molecules in various physical, chemical or biological contexts[2,5–7]. In biology, single-molecule fluorescence techniques, originally introduced for *in vitro* systems[2,8], are now becoming part of the cell imaging toolkit[9]. They are particularly appealing to investigate biochemical reactions in live cells, in which many molecular events are spatially and temporally heterogeneous. When examining a particular molecular process by ensemble methods, information on inhomogeneous behavior, kinetic and reactive variability or local heterogeneity is often lost[2,7,8]. Additionally, biochemical reactions in cells are rarely synchronized, making the characterization of their different kinetic steps difficult from ensemble measurements. For example, consider the case of channel receptors in a cellular membrane. When channels are studied one at a time, important insights on, for instance, fast or slow membrane diffusion owing to differences in channel subunit compositions, variability in channel opening and closing rates or transient association with particular membrane domains can be obtained. All these processes, potentially key to the channel functions, are often inaccessible or blurred in ensemble measurements.

For investigations in cells, an additional—and often overlooked—argument holds in favor of single-molecule approaches. Many key cellular processes are mediated by a small number of molecules and, thereby, can be viewed as single-molecule events. For instance, signal transmission at neuronal synapses depends on the response of a few (10–100) receptors for neurotransmitters in the synaptic cleft. Similarly, regulation of gene expression relies on the activity of transcription factors, often present in limited numbers in the cell nucleus. Single-molecule imaging is thus expected to provide a more faithful view of dynamic endogenous systems compared to methods, such as fluorescence recovery after photobleaching, that involve the overexpression of labeled molecules. In the latter case, a large increase in molecular concentration might shift biochemical equilibria, with the risk of altering the kinetic parameters of the cellular networks under study[10].

QDs as probes for single-molecule imaging in cells

Because of its sensitivity, specificity, noninvasiveness and spatial resolution, fluorescence microscopy is a favored tool in single-molecule research. Organic dyes and fluorescent proteins along with QDs are the predominant types of fluorophores applied for labeling single molecules[2,7,9]. From this toolkit, the photophysical merits of the fluorophore must be matched with the requirements of the intended application. An extensive comparison of the photophysical properties of QDs and dyes is presented in reference 11. QDs have important additional advantages over dyes or fluorescent proteins for single-molecule *in vitro* assays (reviewed in ref. 12) and live-cell experiments. Specifically, QDs have very high brightness owing to their extinction coefficient, which is at least ten times larger than that of the best dyes. This facilitates the imaging of individual QDs with high signal-to-noise ratio (SNR), even with standard epifluorescence microscopes[5,6] (for practical considerations, see **Box 1**) and allows the precise localization of individual QDs within a few nanometers, well below the diffraction limit (~250 nm). Just as important is the high resistance to photobleaching of the QD fluorescence signal, which is several orders of magnitude larger than for dyes or fluorescent proteins and enables the study of QD-labeled molecules for extended durations (tens of minutes to hours). When observed at the individual level, a remarkable feature of QDs is their propensity for fluorescence blinking[13]. Under continuous excitation, the QD fluorescent signal randomly alternates between bright and dark levels (**Fig. 1**). As blinking is absent in ensemble measurements, it can be beneficial as a criterion for identifying individual QDs but it complicates data processing because trajectories of labeled molecules must be reconstructed from a transiently vanishing signal.

Although the optical advantages of QDs for single-molecule experiments are clear, their colloidal and biochemical features must also be taken into consideration. A QD probe is a hybrid organic-inorganic system, which contains a semiconductor nanoparticle surrounded by biocompatible surface coatings and functional biomolecules (**Fig. 1**). The optical properties of QDs are determined by the inorganic nanoparticle, and they generally scale with the QD size (2–10 nm)[14]. QDs formed from a cadmium selenide (CdSe) core and a zinc sulfide (ZnS) shell have been extremely popular for biological imaging because the fluorescence emission can be tuned over the entire visible spectrum, and the synthesis of this material is well optimized[15]. Because the synthesis typically occurs in hydrophobic solvents, treatment with amphiphilic or hydrophilic surface coatings is necessary to enable QD biocompatibility (for a review, see ref. 16). The final component of an active QD probe is the functionalized surface that promotes specific interactions with biological targets. Functionalization is typically achieved by conjugating reactive biomolecules[16] (enzymes, antibodies, nucleic acids and others) (**Fig. 1**) and poly(ethylene glycol) (PEG), which is often necessary to minimize nonspecific interactions of the QD with biological material[17,18].

The complex architecture of QD probes has long posed considerable technical hurdles for many who were interested in using this technology. However, recent commercialization of QD probes suitable for diverse biological imaging applications, including SQT, has greatly facilitated their use. Commercial QDs are now available with various reactive functionalities, including streptavidin or secondary antibodies. Yet despite the growing use of these QDs, they do have limitations that become relevant for SQT. For instance, surface coatings on commercially available QDs are often bulky, consisting of amphiphilic molecules, PEG and multiple copies of antibodies or proteins (polyvalency), all contributing to a hydrodynamic diameter (D_h) on the order of ~20–40 nm[19]. The large size of these QDs places restrictions on studying spatially confined or crowded regions of the cell and may also perturb the behavior of the labeled molecules. For instance, the size of some commercially available QDs was shown to impair their ability to access the cleft at excitatory neuronal synapses[20,21]. When compared directly with small dyes, these QDs were observed to slow down the membrane diffusion of glutamate receptors[21] and to change the type of motion of potassium channels[22]. Another issue is the polyvalency of commercially available QDs, which may induce the cross-linking of labeled molecules and possibly bias the observed mobility, trigger internalization of membrane targets or activate signaling cascades.

Reducing size and controlling valency. The limitations imposed by the size and polyvalency of commercially available QDs have

motivated the engineering and development of new surface coatings and bioconjugation strategies. Reducing QD size has proven difficult because decreased colloidal stability and increased nonspecific interactions often accompanies any size decrease. One approach suitable for SQT relies on the encapsulation of QDs in PEGylated micelles, which results in QDs that are slightly more compact than commercially available QDs (D_h of ~15–20 nm)[23–25]. A surface coating based on PEGylated monothiols (D_h of ~11 nm) was used for SQT of membrane lipids[26], but may have limited use because of the instability of monothiol coordination to the QD surface[27]. Dihydrolipoic acid (DHLA)-PEG and engineered peptides are two particularly interesting surface coatings that yield highly monodisperse, stable and compact QDs, with half the size (D_h of ~10–14 nm) of commercially available QDs. The former has been developed based on DHLA attached to short linear chains of PEG[18,28]. The key feature is stable coordination of dithiols to the QD surface, which does not suffer from the instability of monothiols. Good performance of DHLA-PEG–based QDs in cell imaging[18] and SQT[20] has also been established. The engineered peptide surface coating is based on two-domain commercially available peptides[29,30], which has also been validated for SQT of many cellular targets[30–32]. The engineered peptides contain a cysteine-rich adhesive domain that is stably anchored to the QD surface by multithiol coordination and a second domain containing PEG and hydrophilic amino acids. The QD reactivity can be adjusted by mixing and matching different functional peptides at the surface[29].

BOX 1 FREQUENTLY ASKED QUESTIONS ABOUT SQT

How are imaging conditions optimized? For single-QD detection, widefield epifluorescence microscopy is always preferred over raster scan–based methods such as confocal microscopy (see ref. 5 for details on instrumentation). When using a microscope with an immersion objective (numerical aperture > 1.3) and a sensitive camera (such as a cooled electron-multiplied charge-coupled device (CCD)), acquisition times as short as 1–10 ms per frame can be achieved while maintaining a good SNR. Total internal reflection fluorescence microscopy (TIRF) can be used to enhance the SNR when the QD-labeled molecules are located within ~200 nm of the coverslip, such as in the cell basal membrane.

The objective magnification, M, should be set such that the PSF is correctly sampled on the camera detector but does not spread over too many pixels to limit unnecessary noise. An effective pixel size (camera pixel size divided by M) around 100 nm is generally an appropriate choice that satisfies Nyquist criterion.

Which excitation source, wavelength and intensity should be used? The wide absorbance and large extinction coefficient, ε, of QDs enables much flexibility in the choice of excitation sources. Lamps (mercury, xenon or metal halide), light-emitting diodes (LEDs) or lasers can all be used to excite QDs. As ε increases at higher energy, the QD signal can be enhanced by selecting an excitation wavelength in the ultraviolet–blue region (350–400 nm). However, this may lead to increased cellular autofluorescence and can also be harmful to live cells. In practice, a better SNR is often achieved with excitation in the green–orange region (530–580 nm).

The excitation intensity should always be kept to the minimum value compatible with the desired SNR and acquisition time because QD blinking rates are enhanced at higher excitation intensities. For laser excitation, an intensity of ~0.5 kW cm^{-2} is generally appropriate.

What color QD should be used? If possible, we recommend using QDs with an emission wavelength in the red region (600–700 nm), a spectral region where the cellular autofluorescence is often reduced. Red-emitting QDs also facilitate multicolor detection of QDs and GFP-tagged proteins using a single excitation source in the blue region (for example, a 488 nm laser). Another important consideration is that at wavelengths longer than 700 nm, the detection efficiency of CCD cameras is substantially diminished.

For two-color QD imaging and tracking, QDs with well-separated emission wavelengths should be chosen. Owing to the generally narrow emission band of the probes, this is easily achieved in the red spectral region, which is optimal for SQT. QDs emitting at 605 and 655 nm or above provide a good combination, with little spectral overlap in emission, and facilitate excitation with a single light source. To take full advantage of the nanometer positioning accuracy of SQT in such dual-color QD experiments, it is important to obtain good alignment of the images formed in both detection channels. Multifluorophore-loaded beads emitting in both channels can be imaged to align the channels and correct for possible distortion and chromatic aberrations.

How is nonspecific QD binding to cells limited and specific labeling density optimized? Nonspecific binding of QDs to biological samples and the coverslip surface is the main source of difficulty in SQT experiments. Although there is no universal solution, the following recommendations often help to reduce the nonspecific binding. First, QDs incorporating PEG into their surface coatings should be used, because PEG is very effective at reducing these interactions. Second, a careful choice of buffer conditions can largely reduce the nonspecific interactions. A borate buffer supplemented with 2% (wt/vol) bovine serum albumin or 0.5% casein often provides the best results (see ref. 33). For tracking, it is important to obtain an appropriate density of specifically labeled molecules. If the fluorescent spots are too close, individual trajectories of the diffusing molecules will tend to cross too often, making the subsequent analysis complex and time-consuming. Yet a sufficient labeling density aids in sampling the whole cell. As the affinity of the QD conjugate and the expression level of the target determine the overall labeling efficiency, optimal labeling conditions must be empirically determined by adjusting concentrations (typically nanomolar range), incubation time (seconds to minutes), temperature or media composition.

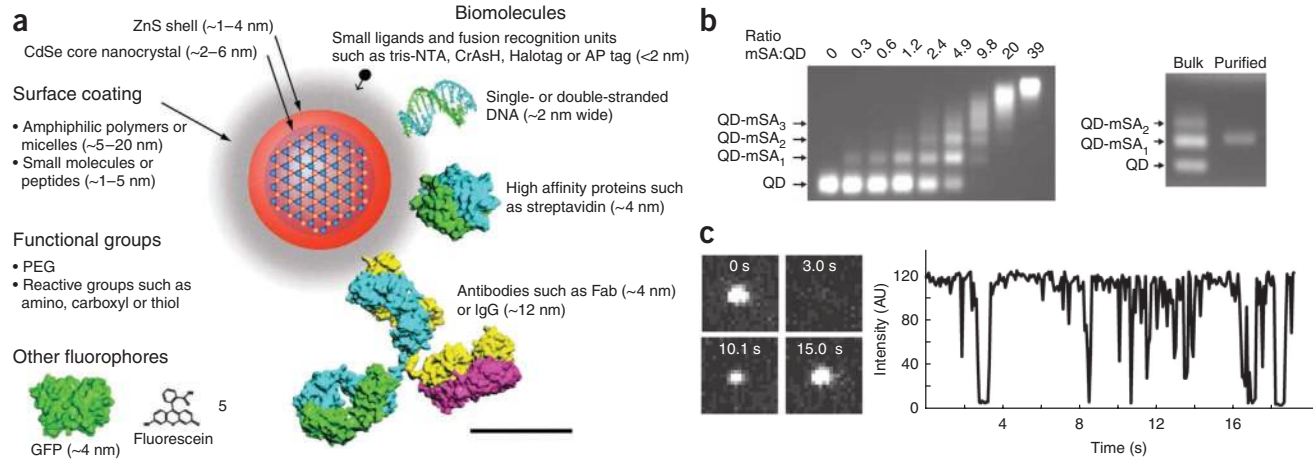

Figure 1 | Structure and properties of QD probes. (**a**) Schematic representation of a QD probe. The inorganic CdSe core nanocrystal and ZnS shell (red) dictate the optical properties in a size-dependent manner. Organic surface coatings (gray) such as small molecules, peptides and amphiphilic micelles or polymers provide colloidal stability in biological buffers. Key features of the surface coating include PEG to reduce nonspecific interactions and reactive groups to enable conjugation of biomolecules. Biomolecules such as DNA, streptavidin and antibodies are conjugated to the surface to enable specific binding to biological targets. GFP and fluorescein dye are shown for size comparison. Scale bar, 5 nm. (**b**) Preparation of monovalent streptavidin (mSA)-conjugated QDs using separation by agarose gel electrophoresis. Streptavidin is engineered with a single biotin binding site and a polyhistidine sequence that binds to the ZnS surface of QDs. Titration with QDs leads to the formation of discrete bands in the gel corresponding to QDs with exactly 0, 1, 2 and more copies of the engineered streptavidin, which are subsequently purified from the bulk mixture. Reprinted from reference 20. (**c**) Typical fluorescence images of a single QD showing changes in emission intensity (AU, arbitrary units). The intensity time trace illustrates the random alternation between 'on' and 'off' states, known as blinking, which is a signature feature of an individual QD.

Functionalization of QDs mediates specific binding to cellular targets, which is typically achieved by noncovalent or covalent conjugation of reactive biomolecules to the surface. Practically, for SQT, the binding partners must interact with high-affinity (typically dissociation constant, K_D better than nanomolar) to ensure that the binding time is longer than the required observation time. Thus, the extremely high affinity and stability of the biotin-streptavidin system (K_D, about femtomolar; half-life, greater than several days) has contributed to the popularity of streptavidin-functionalized QDs for SQT. These streptavidin-functionalized QDs are often used through a biotinylated antibody mediating the binding to endogenous targets[33] or to small genetically engineered fusion tags in the target such as hemagglutinin (HA)[10] or c-myc[34,35]. This approach is well-suited for multicolor SQT of the same[36,37] or multiple targets[38]. However, a disadvantage is that antibodies are large, divalent and sometimes have poor affinity. New targeting approaches are emerging that eliminate the need for traditional antibodies altogether, which include a variety of high-affinity fusion tags and binding partners initially developed for site-selective and stable labeling of cellular molecules with fluorophores (for a review, see ref. 39). For instance, streptavidin-functionalized QDs can be directly applied after enzymatic biotinylation of a target carrying an acceptor-peptide (AP) fusion tag[20,40]. Biological imaging of QDs, and in some cases SQT, has already been achieved by expression of avidin[29], CrAsH[41], Halotag[42], polyhistidine[24,43] and single-chain antibody[32] fusions to cellular targets followed by labeling with QDs functionalized with the corresponding binding partner. These complementary and orthogonal labeling approaches not only enable more flexible experimental designs, such as the ability to site-selectively position the fusion tag, but they also facilitate multicolor SQT, which was demonstrated by combining the AP and polyhistidine fusions[24]. Several studies have now found that QDs can alter interactions between binding partners, for instance, by negatively influencing the K_D and half-life[32,44]. One way to circumvent this issue is to depart from noncovalent targeting strategies and to covalently attach QDs, which has been accomplished for the cutinase fusion tag[45] or carrier protein fusions combined with coenzyme A[46,47]. Extension of these covalent approaches to SQT could be particularly interesting for applications requiring very long observation.

Regardless of the targeting scheme, reducing the polyvalency of QDs is important for SQT applications. The QDs' large surface area to volume ratio provides many points of attachment for conjugated biomolecules (up to ~10 streptavidin molecules or antibodies per QD; **Fig. 1**). Because of the reduced size and high monodispersity of QDs with compact surface coatings, better control over the stoichiometry of conjugated biomolecules can now be achieved. Notably, QDs containing exact numbers of biomolecules (0, 1, 2, 3 and so on) can be resolved as discrete populations using separation and purification by agarose gel electrophoresis (**Fig. 1**). This method, first developed for gold nanoparticles[48], has been applied to prepare monovalent QD probes conjugated to a single copy of an antibody, an engineered streptavidin with a single biotin binding site[20] or a functional PEG[49]. Monovalent QD probes eliminate the risks of target cross-linking and are also smaller. These advantages have been highlighted by showing that smaller QD probes can enter the size-restricted neuronal synapse more efficiently that commercially available QDs[20]. The combination of compact surface coatings, high-affinity binding partners and functional monovalency currently reflect the state of the art in design of small QD probes for SQT.

Processing and analysis of single-QD tracking data. In addition to optimizing QD size and valency, another important aspect of SQT is to efficiently process large datasets. In most cases, the raw data from SQT experiments comprise a two-dimensional series of time-lapse images acquired by the microscope camera.

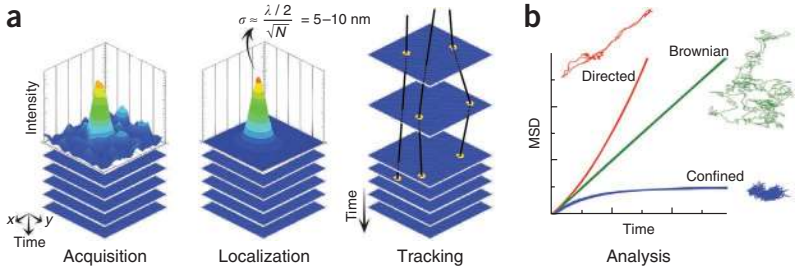

Figure 2 | Processing and analysis of SQT data. (**a**) To build trajectories of diffusing QDs, first, raw data collected at the microscope camera (acquisition) are exported as a two-dimensional series of images encoding fluorescence intensity and position. Frame by frame, the center of each diffraction-limited fluorescent spot corresponding to an individual QD is located by Gaussian fitting of the intensity profile (localization). The localization accuracy, σ, is determined by the emission wavelength, λ, and the total number of detected photons, N. Finally, trajectories are formed by connecting spot positions across frames within the entire image series (tracking). Specific correspondence difficulties arise when the density of spots is high or when the fluorescent signal is lost during QD blinking. (**b**) Classification of single-molecule trajectories using the mean squared displacement (MSD) (analysis). The mode of motion can be classified as Brownian motion (such as random diffusion in the membrane), as confined motion (such as entry into membrane domains) or as directed motion (such as linear transport owing to molecular motors) depending on the shape of the MSD function over time.

When the density of the labeled molecules is low enough, each QD appears as an isolated fluorescent spot corresponding to the diffraction-limited point spread function (PSF) of the microscope (**Fig. 2**). A quantitative analysis of the motion of the spots requires reconstruction of the individual trajectories from the raw data. A common approach is to sequentially analyze each frame of the image stack in a two-step procedure: first, spots are detected and localized, and then correspondence between frames is established[50]. In single-molecule imaging, localizing individual spots is possible with a precision not limited by diffraction, but rather by the SNR in the data[51]. The spot center is usually located by Gaussian fitting of the PSF intensity profile[51,52]. Owing to the superior brightness of QDs, the pointing accuracy is often determined by the total number of detected photons (**Fig. 2**) and can be as low as 10 nm for a 10-ms integration time. After localization, trajectories are formed by linking the centers of fluorescent spots across adjacent frames in the image series. In the case of QDs, blinking of the fluorescent signal raises specific difficulties of correspondence between the frames. Several methods have been implemented to track multiple transiently disappearing targets[50,53–55]. Two recently reported algorithms performed robustly on densely populated simulated and experimental data and can be freely downloaded, which should be an attractive option for many groups interested in this type of analysis[54,55]. Overall, the ability to process trajectories in a high-throughput manner, using semi-automatic algorithms, now enables large datasets to be analyzed within a (relatively) rapid time window.

Various analysis techniques have been developed to extract meaningful properties from the trajectories of single molecules. In general, computing the mean square displacement as a function of time permits a rapid determination of the mode of motion (diffusive, directed, confined and others) and yields associated parameters (diffusion coefficient, transport velocity, size of confinement domain and others)[1,7,56] (**Fig. 2**). This method, however, only provides averaged motion parameters over the entire trajectory. Thus, mean square displacement analysis might be inadequate to describe transient behaviors when a molecule dynamically interacts with specific molecular partners or with its direct environment. This is the case, for instance, when a diffusing membrane molecule is temporarily confined in a microdomain[31] or when a protein is transported after transient attachment to a molecular motor or to cytoskeletal elements[57]. Given the long trajectories now accessible in SQT experiments, a local, rather than global analysis is often preferable. More advanced computational techniques have thus been devised to analyze situations in which a molecule alternates between multiple types of movement[31,57–61] or to extract information about the shape of the local energy landscape[62]. An alternative approach altogether has been demonstrated using image correlation spectroscopy[63], which does not rely on the formation and analysis of individual trajectories. Although this method is less demanding in terms of processing time, it is potentially less informative because it provides only population-averaged values of the kinetic parameters (diffusion coefficient, velocity and others).

SQT studies of membrane dynamics and organization

In many biological systems, the implementation of SQT has provided insight into mechanisms that contribute to the localization and the mobility of molecules in live cells. So far most of the experiments have focused on analyzing the diffusion dynamics of plasma membrane molecules, which, often, can be easily targeted (**Fig. 3**). Tracking and quantifying the movement of QD-labeled proteins such as EGF receptor[36,64] GABA receptor[65], potassium channels[66,67], CFTR channels[10,68], integrins[69] or band 3 proteins[70] indicated that cytoskeletal elements such as actin or microtubules actively participate in the distribution and constrained diffusion of many membrane proteins. SQT on aquaporins indicated that these water channels generally diffuse freely in cell membranes, although certain isoforms appeared to be highly confined in large protein domains[34,71,72]. Additional information can be gathered by directly correlating the diffusion dynamics of QD-labeled molecules with the actual position of membrane structures labeled with dyes or fluorescent proteins. For instance, simultaneous imaging of QD-tagged proteins together with actin[38], with lipid microdomains[31], with membrane cavities[31] or with clustered protein domains[67] has shown how these structures strongly influence lateral dynamics in living cells (**Fig. 3**). SQT analyses with two (or more) colors of QDs can also reveal fine protein-protein interactions in membranes. Although in some instances the large size of QDs might hinder direct interactions, two-color SQT has already been implemented to image EGF receptor complexes[36] and amyloid precursor protein (APP) dimers[37]. Measuring the correlated diffusion of molecules labeled with distinguishable QDs is a powerful criterion to discriminate between true receptor dimerization and random co-localization or simultaneous entry in a shared membrane domain.

In neuroscience, SQT has greatly facilitated the direct measurement of the mobility and entry-exit kinetics at synapses for a variety of neuroreceptors, including AMPA[21,73], NMDA[74],

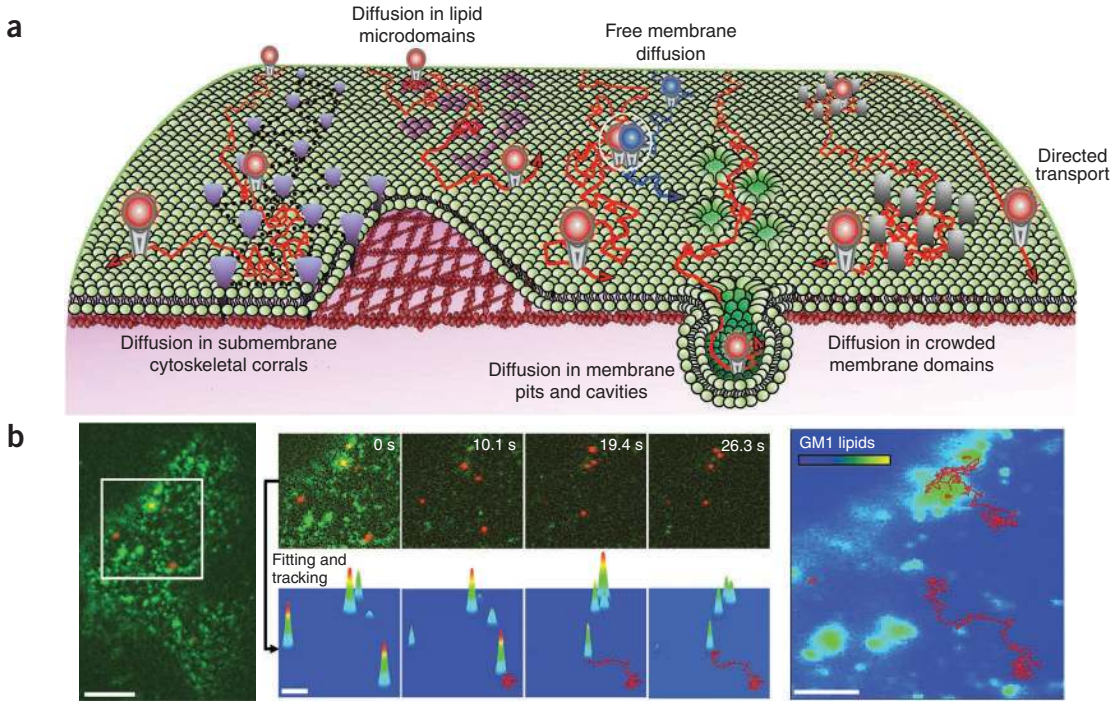

Figure 3 | Studying membrane dynamics and organization by SQT. (**a**) Schematic representation of diverse lateral diffusion for plasma membrane lipids or proteins detected by SQT. Constrained membrane diffusion can be induced by a variety of structures and microdomains, including submembranous skeleton corrals, lipid microdomains, membrane pits and cavities, crowded membrane domains or sites of protein/protein interactions (white circle). (**b**) An example of multicolor imaging and SQT. Simultaneous imaging of QD-tagged lipid raft-associated proteins (red) and GM1 glycosphingolipid-rich microdomains (green) in the plasma membrane of HeLa cells was done by total internal reflection fluorescence microscopy. Diffusion trajectories of individual raft proteins were determined by fitting the QD fluorescent spots (red) in each image for the entire time series (magnification of the boxed area in the image on the left). These trajectories were then overlaid on the intensity projection image of the GM1 lipids to correlate the protein diffusion paths with the position of lipid microdomains. Scale bars, 7 μm (left), 1 μm (middle) and 2 μm (right). Reproduced with permission from reference 31.

glycine[4,35,75], GABA[75], cannabinoid[76] and acetyl choline receptors[77] (for a review, see ref. 78). Such analyses have also shed light on mechanisms by which the local concentration and the mobility of neuroreceptors can be modified, such as during interactions with cytoskeletal structures[79], the extracellular matrix[80], membrane domains[81] or owing to synaptic activity[73,75]. SQT experiments have reinforced the notion that neuronal surface mobility and its regulation are among the key molecular bases of synaptic plasticity, complementing previous views focused on endo- and exocytotic processes[78]. SQT can also be used to directly study these processes, underscoring the high versatility of the technique. For instance, the controversial issue of synaptic vesicle 'kiss-and-run' versus full vesicular collapse was examined by SQT during neuronal stimulation. A careful choice of QD size and charge permitted the labeling of single presynaptic vesicles and the observation of fusion processes in response to synaptic excitation[82,83] (**Fig. 4**).

Membrane diffusion studies have motivated the extension of SQT to intracellular targets involved in signaling, transport or gene regulation. Technically, this requires overcoming the challenges of delivering QDs across the plasma membrane (**Box 2**), an issue that has not yet been fully solved. Nevertheless, the superior optical properties of QD probes permit real-time visualization of cellular internalization pathways and long-term tracking of molecules directly inside cells (**Fig. 5**). In particular, QDs functionalized with receptor ligands provide means to both activate membrane receptors and follow their intracellular fate. In the case of EGF[36,64] and NGF[84–86] ligands, SQT has revealed some details about the complex internalization mechanisms of growth factor receptors in endosomes, including heterogeneous endosomal transport rates and retrograde transport (**Fig. 5**). Similarly, QD labeling of individual viruses, which has already been achieved[87], may facilitate the visualization of various steps in the infection process, from cell membrane binding and internalization to intracellular disassembly of the virus.

A few SQT experiments have started to investigate the properties of intracellular molecules, aside from those actively internalized at the membrane. The first systems were kinesin-1 (ref. 88) and myosin-V[89,90], two motor proteins involved in cellular transport and cell division. Once labeled molecules are loaded in the cytosol via a pinocytotic technique, the velocity and processivity of single QD-labeled motors could be accessed directly in live cells[88–90] (**Fig. 5**). The brightness of QDs also made it possible to observe individual 36-nm steps of myosin-V motors walking hand-over-hand along F-actin filaments[89,90]. More recently, non-functionalized QDs were used to analyze cytosolic fluid flows in moving cells[91]. Beyond crossing the plasma membrane, accessing the cell nucleus with QDs presents additional technical barriers because the probes must also pass the nuclear envelope and navigate within this extremely crowded environment. Preliminary SQT studies already have shown that it is possible to directly microinject QD-labeled mRNAs in the nucleus of living cells[92], revealing that they were preferentially partitioned in the interchromatin space.

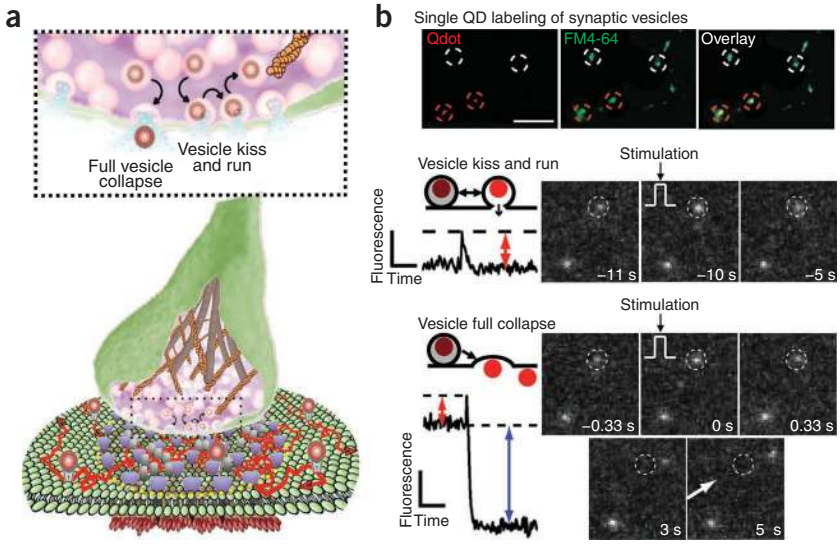

Figure 4 | Synaptic biology with QDs. (**a**) Schematic representation of a synaptic bouton packed with vesicles, some of which are loaded with individual QDs. Vesicular release can take place by full vesicle collapse or kiss and run at the plasma membrane. On the postsynaptic site (yellow delimitation), molecular crowding, cytoskeletal scaffolding and anchoring of membrane proteins can hinder the mobility of QD-labeled neuroreceptors and regulate their activity. (**b**) An example of SQT to study synaptic vesicle fusions during neuronal stimulation. Single QDs were loaded into synaptic boutons (labeled with FM4-64). Changes in QD fluorescence signal report on pH modification in a synaptic vesicle as it fuses with the plasma membrane. Brief membrane fusion during vesicle kiss and run was characterized by a transient increase in QD fluorescence that followed stimulation. Vesicle full collapse fusion, however, was detected by an initial increase in QD signal followed by a vanishing fluorescent signal as the QD diffused away from the fusion site in the direction of the white arrow. For the same vesicle, both kiss and run (time, –10 s) and full collapse fusion (time, 0 s) were observed at different stimulation. Although the interpretation of these data have been subjected to some controversy, high-frequency stimulations at synapses generally appear to correlate with increased likelihood of kiss-and-run fusions, whereas low-rate steady-state neuronal stimulations more often induced full collapse fusions. Reprinted from reference 83 with permission from the American Association for the Advancement of Science.

Challenges and prospects

Despite the success of many SQT experiments in live cells, important methodological issues still need to be addressed in terms of optical imaging, processing and QD probe synthesis and functionalization.

Three-dimensional QD tracking. So far, most SQT experiments collect raw data as a time series of two-dimensional images. This is an obvious limitation in many situations in which three-dimensional tracking is preferable, for instance, when tracking cytoplasmic or nuclear targets. Three-dimensional tracking

BOX 2 DELIVERING QUANTUM DOTS INTO CELLS

Crossing the cellular membrane with QDs remains a difficult challenge in live cells. Toward this goal, many protocols have been developed to deliver QDs into the cytoplasm (for a detailed review, see ref. 108). Delivery methods most relevant for intracellular SQT can be broadly classified into three categories, as follows.

Delivery via endocytotic mechanisms. Incubation of cells with QDs in the external medium often leads to the internalization of QDs by nonspecific endocytosis, depending on factors such as the QD size, surface coating, concentration, cell type and the duration of incubation[109,110]. Endocytosis can be enhanced by functionalizing the QD surface with short peptides, known for the ability to cross cell membranes[111,112]. In the case of receptor-mediated endocytosis, receptors on the cell membrane recognize and internalize QDs that have been functionalized with binding partners, such as proteins, small molecule ligands[36,64,84,85,95,109,113,114] or viruses[87]. Endocytotic methods have the disadvantage that internalized QDs are often trapped within endosomal compartments, which may block their ability to reach specific intracellular targets.

Lipid- and polymer-mediated delivery. An alternative strategy for internalization relies on enhancing the membrane permeability of QDs via encapsulation or surface modification. Encapsulation of QDs in cationic lipid micelles, such as those formed from DNA transfection reagents or in biodegradable polymeric capsules, has been shown to facilitate delivery of QDs[110] in some cases to specific intracellular targets[115,116]. Another encapsulation method applies osmotic shock to release QDs from pinocytotic vesicles delivered into the cytoplasm, which is a technique that has already proven successful in several SQT applications[88,89]. Alternatively, direct modification of the QD surface to enhance their membrane permeability can be accomplished by functionalization with cationic polymers[117,118], which can escape from vesicles once they are internalized, or with certain peptides that bypass endocytotic mechanisms altogether[119].

Forced delivery. A distinctly different delivery approach uses mechanical manipulation of the cell membrane. Typically, this is achieved by direct microinjection of QDs into the cytoplasm[23,92,110] or nucleus[92] from a thin glass needle loaded with QDs or by electroporation[91]. Microinjection has the primary advantage that the QDs are individually dispersed at the injection site, which is a critical requirement for SQT. However, limitations include the serial aspect of the technique and its potentially disruptive effect to cells. A promising advance is the use of carbon nanotubes in place of glass needles for injection of QDs[120] because the smaller size of nanotubes reduces damage to the membrane at the injection site. Notably, parallelization of QD injection across multiple cells can now be achieved by engineering surfaces with arrays of the nanotubes[121].

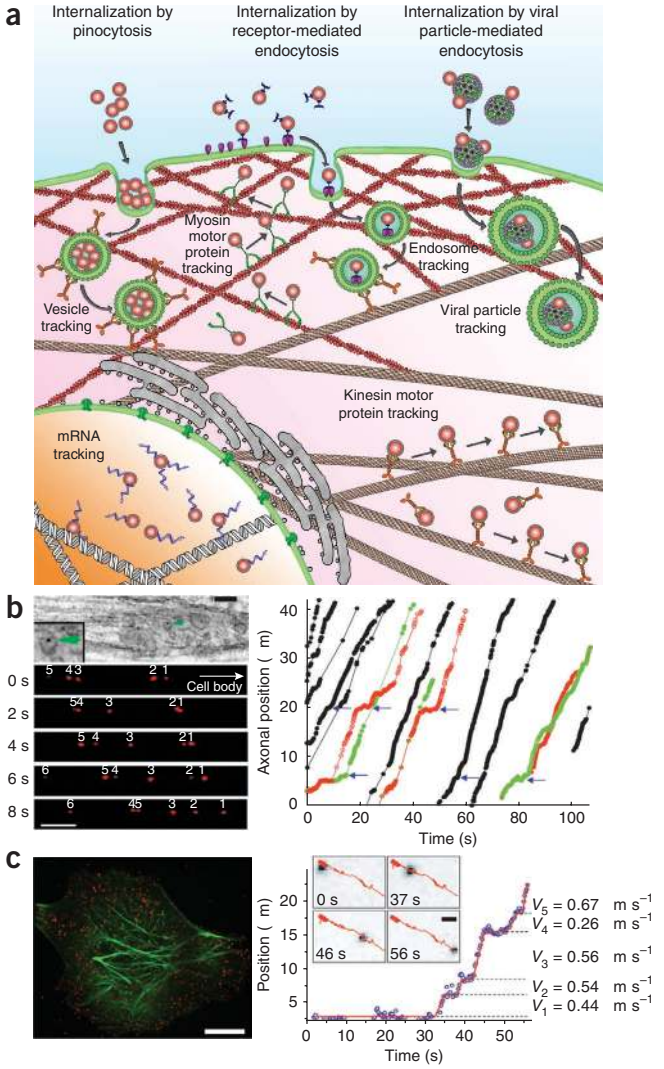

Figure 5 | Intracellular tracking of QDs. (**a**) Schematic representation of various internalization pathways and intracellular dynamics studied by SQT, including motor protein movements, endosome retrograde transport, viral particle trafficking and mRNA intranuclear diffusion. (**b**) Active retrograde transport of endosomes containing single QD-labeled nerve growth factors after internalization in culture neurons. Endosomal localization and movements along axons toward the cell body confirmed by electron microscopy and SQT (left). Scale bars, 0.2 µm (top) and 5 µm (bottom). Trajectory analysis (right) indicating that different endosomes within the same axon can move independently (black) or move together and pass other endosomes (red and green). Transport pausing at the same axonal locations for different endosomes is indicated by blue arrows. Reprinted from reference 84 with permission from the National Academy of Sciences. (**c**) SQT of motor proteins in the cytoplasm of HeLa cells. Spinning disk fluorescence image of myosin-labeled QD (red) and phalloidin-labeled actin filaments (green) in the cytoplasm of a fixed HeLa cell after QD internalization by pinocytotic influx (left). Reprinted from reference 89 with permission from Elsevier. Tracking of a single QD-labeled kinesin moving along a microtubule (inset) gives access to the velocity and the processivity of the motor protein in live cells (right). Scale bars, 10 µm (left) and 1 µm (right). Reprinted from reference 88 with permission from the American Chemical Society.

will be even more of an issue in the future when SQT experiments are performed in thick multicellular systems (tissues, neuronal slices and others). Overall, the development of accurate methods to localize and track fluorophores in three dimensions is an objective common to many imaging applications in biology, and several of them have already been used to track QDs in cells. Tracking can be done with either point-scanning[93] or widefield epifluorescence excitation. In the latter case, which is experimentally simpler, the position along the *z* axis is obtained with a resolution of ~50 nm by imaging nanoparticles with an astigmatic lens[94] or with a multifocal plane setup[95], or by engineering a double helix PSF[96]. However, the use of these methods has been essentially limited to proof-of-concept experiments. Moreover, the widefield techniques function over depths that do not exceed a couple of micrometers, not yet compatible with the size of a cell (~10–20 µm). Much work remains necessary to achieve versatile optical techniques and efficient processing tools capable of tracking multiple QDs in an entire cellular volume, while accounting for photophysical effects such as blinking.

Further reducing QD size with novel materials. Although considerable progress in surface chemistry engineering has led to reduced-size CdSe-ZnS QDs (D_h of ~12 nm, equivalent to a ~400 kDa complex), these probes are still large compared to many molecules and might affect the activity or mobility of targets after labeling. Experiments in small animals have also emphasized how the biodistribution of QDs through tissues critically depends on their size and colloidal properties[97]. A promising way to prepare smaller QD probes is to depart from the CdSe-ZnS material altogether and to take advantage of the vast choice of semiconductor materials and modern methods of nanoparticle engineering[15]. For instance, the synthesis of CdTe QDs is now well developed, and these QD probes can be prepared with D_h as small as 6 nm[98]. The use of InP and InAs QDs, coated with a ZnS shell, is also an appealing possibility, with demonstrated synthesis methods and D_h of 5–8 nm[99,100]. These QDs have tunable fluorescence from the visible to infrared, which is both an advantage for multiplexing and a constraint because cameras tend to be less sensitive in the infrared spectral region. Perhaps the largest hurdle in using these alternative materials for SQT experiments is that control of the photophysical and surface properties is somewhat preliminary. In particular, additional effort is required to match these materials with the surface coatings and conjugation strategies that have been recently developed for CdSe-ZnS QDs.

Eliminating blinking. Blinking was long thought to be an inescapable property of individual QD fluorescence. From a theoretical perspective, the origins of blinking remain somewhat controversial, although many models attribute the off state to charging of the QD[13]. It was initially observed that a high concentration (>50 mM) of small thiol molecules was sufficient to reduce blinking of commercially available QDs[101], but these are unsuitable conditions for live cells. Two reports have since shown that QDs with greatly reduced blinking can be obtained through accurate control of the inorganic shell[102,103]. The critical step is to grow very thick shells (up to 20 monolayers of CdS or CdZnS) while reducing the lattice mismatch between the CdSe core and the shell material. This results in fewer charge carrier trap states and limits blinking. A disadvantage for SQT with these reduced-blinking QDs is that the final diameter of the inorganic material is 15–20 nm. Very recently, completely nonblinking QDs

with a diameter of 8 nm were synthesized with a CdSe core and ZnSe shell, with Zn gradually alloyed into the core[104]. However, these nonblinking QDs have a multipeak fluorescence emission, which might be a limitation for multicolor experiments. Despite their relative drawbacks, these new QDs represent an attractive option for SQT because it would no longer be necessary to account for blinking during image processing and analysis.

Targeting intracellular proteins. The most important open challenge in SQT is probably the ability to directly target specific populations of molecules inside the cell. The difficulty for nanoparticles to pass through the plasma membrane therefore constitutes a major obstacle for many applications of SQT, and therefore development of versatile methods that allow efficient delivery of these particles is still necessary (**Box 1**). A second problem is the targeting strategy itself. So far, SQT of intracellular single molecules has been limited to biomolecules (such as mRNAs or molecular motors) produced and conjugated to QDs *in vitro* before internalization. In many cases, though, it would be preferable to study endogenous intracellular molecules rather than expressing and conjugating them *in vitro*, which can be technically demanding or impossible. In contrast to membrane labeling, internalized QDs that do not bind to their target cannot be simply washed away, making it difficult to differentiate between bound and unbound QDs. The use of fusion tags and high-affinity binding partners should help alleviate this issue in the future. Intracellular delivery and targeting will also necessitate accounting for QD size and charge, two critical factors governing the behavior of nanoparticles inside cells. Altogether, only a combined optimization of the QD colloidal and biofunctional properties can successfully address these complex issues.

Conclusion

A growing number of single-molecule and single QD experiments have shown how important parameters (diffusion, transport, association constants and others) governing molecular interactions can now be directly accessed in live cells. Such *in situ* biochemical measurements take into account many factors that cannot be faithfully reproduced *in vitro*, such as molecular crowding, dimensionality, heterogeneous concentrations of reagents or the local chemical environment. In many cases, SQT measurements have pointed to the transient, and often elusive, nature of molecular interactions. These observations are consistent with the view that supramolecular assemblies (such as the synapse) are not static structures but in constant turnover[105]. Yet how robust self-organization forms and is maintained despite—or thanks to—the heterogeneities and fluctuations observed at the molecular scale remains an open question. Addressing this issue is probably one of the most exciting prospects brought by SQT techniques. This task will also benefit from an often overlooked aspect of single QD imaging, namely the facility with which many single molecules can be simultaneously monitored. Not only does the parallel acquisition increase the statistical throughput, but it also means that QDs can be used as tracers to sample a population. As shown in recent studies on nerve chemotaxis[65], this is a fruitful approach to quantitatively describe how the integrated dynamics of a population emerge from the molecular behavior of its individual components. The dynamic information offered by SQT favorably complements new imaging methods giving access to cellular structure[106] and composition[107] with unprecedented resolution. Combined, they should prove to be a valuable tool to decipher the rules governing the dynamic architecture of live cells and possibly reshape some important conceptual ideas in cell biology.

ACKNOWLEDGMENTS

We thank Y. Bellaiche, G. Cappello, P. Desbiolles, V. Marchi-Artzner, M. Renner and A. Triller for careful reading of the manuscript and valuable discussions. F.P. acknowledges financial support from a Marie Curie-Intra-European Fellowship (contract MEIF-CT-2006-040210) and a European Molecular Biology Organization Long-Term Fellowship. S.C. is supported by postdoctoral fellowships from Université Pierre et Marie Curie and the Fondation pour la Recherche Médicale. A.S. is supported by a doctoral fellowship from the Marie Curie Training Network. M.D. acknowledges funding from the Fondation pour la Recherche Médicale, Agence Nationale pour la Recherche (ANR-05-PNANO-045), the Human Frontier Science Program (RGP0005/2007) and the Centre C'Nano Ile de France.

COMPETING FINANCIAL INTERESTS

The authors declare no competing financial interests.

Published online at http://www.nature.com/naturemethods/.
Reprints and permissions information is available online at http://npg.nature.com/reprintsandpermissions/.

1. Saxton, M.J. & Jacobson, K. Single-particle tracking: applications to membrane dynamics. *Annu. Rev. Biophys. Biomol. Struct.* **26**, 373–399 (1997).
2. Joo, C., Balci, H., Ishitsuka, Y., Buranachai, C. & Ha, T. Advances in single-molecule fluorescence methods for molecular biology. *Annu. Rev. Biochem.* **77**, 51–76 (2008).
3. Bruchez, M., Moronne, M., Gin, P., Weiss, S. & Alivisatos, A.P. Semiconductor nanocrystals as fluorescent biological labels. *Science* **281**, 2013–2016 (1998).
4. Dahan, M. *et al.* Diffusion dynamics of glycine receptors revealed by single-quantum dot tracking. *Science* **302**, 442–445 (2003).
First paper describing QD use to track single receptors in live cells.
5. Walter, N.G., Huang, C.Y., Manzo, A.J. & Sobhy, M.A. Do-it-yourself guide: how to use the modern single-molecule toolkit. *Nat. Methods* **5**, 475–489 (2008).
6. Selvin, P.R. & Ha, T. Single-molecule techniques: a laboratory manual (Cold Spring Harbor Laboratory Press, 2008).
7. Wieser, S. & Schutz, G.J. Tracking single molecules in the live cell plasma membrane-do's and don't's. *Methods* **46**, 131–140 (2008).
8. Weiss, S. Fluorescence spectroscopy of single biomolecules. *Science* **283**, 1676–1683 (1999).
9. Lord, S.J., Lee, H.L. & Moerner, W.E. Single-molecule spectroscopy and imaging of biomolecules in living cells. *Anal. Chem.* advance online publication, doi:10.1021/ac9024889 (17 February 2010).
10. Haggie, P.M., Kim, J.K., Lukacs, G.L. & Verkman, A.S. Tracking of quantum dot-labeled CFTR shows near immobilization by C-terminal PDZ interactions. *Mol. Biol. Cell* **17**, 4937–4945 (2006).
11. Resch-Genger, U., Grabolle, M., Cavaliere-Jaricot, S., Nitschke, R. & Nann, T. Quantum dots versus organic dyes as fluorescent labels. *Nat. Methods* **5**, 763–775 (2008).
12. Pons, T. & Mattoussi, H. Investigating biological processes at the single molecule level using luminescent quantum dots. *Ann. Biomed. Eng.* **37**, 1934–1959 (2009).
13. Stefani, F.D., Hoogenboom, J.P. & Barkai, E. Beyond quantum jumps: blinking nanoscale light emitters. *Phys. Today* **62**, 34–39 (2009).
14. Alivisatos, A.P. Semiconductor clusters, nanocrystals and quantum dots. *Science* **271**, 933–937 (1996).
15. Reiss, P., Protiere, M. & Li, L. Core/shell semiconductor nanocrystals. *Small* **5**, 154–168 (2009).
16. Michalet, X. *et al.* Quantum dots for live cells, *in vivo* imaging, and diagnostics. *Science* **307**, 538–544 (2005).
A review of QD properties and applications for biological imaging.
17. Bentzen, E.L. *et al.* Surface modification to reduce nonspecific binding of quantum dots in live cell assays. *Bioconjug. Chem.* **16**, 1488–1494 (2005).
18. Liu, W. *et al.* Compact biocompatible quantum dots functionalized for Cellular imaging. *J. Am. Chem. Soc.* **130**, 1274–1284 (2008).
19. Doose, S., Tsay, J.M., Pinaud, F. & Weiss, S. Comparison of photophysical and colloidal properties of biocompatible semiconductor nanocrystals using fluorescence correlation spectroscopy. *Anal. Chem.* **77**, 2235–2242 (2005).

20. Howarth, M. *et al.* Monovalent, reduced-size quantum dots for imaging receptors on living cells. *Nat. Methods* **5**, 397–399 (2008).
With reference 40, describes clever engineering of small and monofunctional QDs, a substantial improvement for targeting and tracking single membrane proteins.
21. Groc, L. *et al.* Surface trafficking of neurotransmitter receptor: comparison between single-molecule/quantum dot strategies. *J. Neurosci.* **27**, 12433–12437 (2007).
22. Nechyporuk-Zloy, V., Dieterich, P., Oberleithner, H., Stock, C. & Schwab, A. Dynamics of single potassium channel proteins in the plasma membrane of migrating cells. *Am. J. Physiol. Cell Physiol.* **294**, C1096–C1102 (2008).
23. Dubertret, B. *et al. In vivo* imaging of quantum dots encapsulated in phospholipid micelles. *Science* **298**, 1759–1762 (2002).
24. Roullier, V. *et al.* High-affinity labeling and tracking of individual histidine-tagged proteins in live cells using Ni^{2+} Tris-nitrilotriacetic acid quantum dot conjugates. *Nano Lett.* **9**, 1228–1234 (2009).
25. Lees, E.E., Nguyen, T.L., Clayton, A.H.A., Mulvaney, P. & Muir, B.W. The preparation of colloidally stable, water-soluble, biocompatible, semiconductor nanocrystals with a small hydrodynamic diameter. *Acs Nano* **3**, 1121–1128 (2009).
26. Murcia, M.J., Minner, D.E., Mustata, G.M., Ritchie, K. & Naumann, C.A. Design of quantum dot-conjugated lipids for long-term, high-speed tracking experiments on cell surfaces. *J. Am. Chem. Soc.* **130**, 15054–15062 (2008).
27. Aldana, J., Wang, Y.A. & Peng, X.G. Photochemical instability of CdSe nanocrystals coated by hydrophilic thiols. *J. Am. Chem. Soc.* **123**, 8844–8850 (2001).
28. Susumu, K. *et al.* Enhancing the stability and biological functionalities of quantum dots via compact multifunctional ligands. *J. Am. Chem. Soc.* **129**, 13987–13996 (2007).
29. Pinaud, F., King, D., Moore, H.P. & Weiss, S. Bioactivation and cell targeting of semiconductor CdSe/ZnS nanocrystals with phytochelatin-related peptides. *J. Am. Chem. Soc.* **126**, 6115–6123 (2004).
30. Dif, A. *et al.* Small and stable peptidic PEGylated quantum dots to target polyhistidine-tagged proteins with controlled stoichiometry. *J. Am. Chem. Soc.* **131**, 14738–14746 (2009).
31. Pinaud, F. *et al.* Dynamic partitioning of a glycosyl-phosphatidylinositol-anchored protein in glycosphingolipid-rich microdomains imaged by single-quantum dot tracking. *Traffic* **10**, 691–712 (2009).
32. Iyer, G. *et al.* High affinity scFv-hapten pair as a tool for quantum dot labeling and tracking of single proteins in live cells. *Nano Lett.* **8**, 4618–4623 (2008).
33. Bannai, H., Levi, S., Schweizer, C., Dahan, M. & Triller, A. Imaging the lateral diffusion of membrane molecules with quantum dots. *Nat. Protocols* **1**, 2628–2634 (2006).
34. Crane, J.M. & Verkman, A.S. Long-range nonanomalous diffusion of quantum dot-labeled aquaporin-1 water channels in the cell plasma membrane. *Biophys. J.* **94**, 702–713 (2008).
35. Ehrensperger, M.V., Hanus, C., Vannier, C., Triller, A. & Dahan, M. Multiple association states between glycine receptors and gephyrin identified by SPT analysis. *Biophys. J.* **92**, 3706–3718 (2007).
36. Lidke, D.S., Lidke, K.A., Rieger, B., Jovin, T.M. & Arndt-Jovin, D.J. Reaching out for signals: filopodia sense EGF and respond by directed retrograde transport of activated receptors. *J. Cell Biol.* **170**, 619–626 (2005).
37. Gralle, M., Botelho, M.G. & Wouters, F.S. Neuroprotective secreted amyloid precursor protein acts by disrupting amyloid precursor protein dimers. *J. Biol. Chem.* **284**, 15016–15025 (2009).
38. Andrews, N.L. *et al.* Actin restricts Fc epsilon RI diffusion and facilitates antigen-induced receptor immobilization. *Nat. Cell Biol.* **10**, 955–963 (2008).
39. Marks, K.M. & Nolan, G.P. Chemical labeling strategies for cell biology. *Nat. Methods* **3**, 591–596 (2006).
40. Howarth, M., Takao, K., Hayashi, Y. & Ting, A.Y. Targeting quantum dots to surface proteins in living cells with biotin ligase. *Proc. Natl. Acad. Sci. USA* **102**, 7583–7588 (2005).
41. Genin, E. *et al.* CrAsH—quantum dot nanohybrids for smart targeting of proteins. *J. Am. Chem. Soc.* **130**, 8596–8597 (2008).
42. So, M.-K., Yao, H. & Rao, J. HaloTag protein-mediated specific labeling of living cells with quantum dots. *Biochem. Biophys. Res. Commun.* **374**, 419–423 (2008).
43. Kim, J. *et al.* Ni-nitrilotriacetic acid-modified quantum dots as a site-specific labeling agent of histidine-tagged proteins in live cells. *Chem. Commun.* 2008, 1910–1912 (2008).
44. Swift, J.L. & Cramb, D.T. Nanoparticles as fluorescence labels: is size all that matters? *Biophys. J.* **95**, 865–876 (2008).
45. Bonasio, R. *et al.* Specific and covalent labeling of a membrane protein with organic fluorochromes and quantum dots. *Proc. Natl. Acad. Sci. USA* **104**, 14753–14758 (2007).
46. George, N., Pick, H., Vogel, H., Johnsson, N. & Johnsson, K. Specific labeling of cell surface proteins with chemically diverse compounds. *J. Am. Chem. Soc.* **126**, 8896–8897 (2004).
47. Sunbul, M., Yen, M., Zou, Y. & Yin, J. Enzyme catalyzed site-specific protein labeling and cell imaging with quantum dots. *Chem. Commun.* 2008, 5927–5929 (2008).
48. Zanchet, D., Micheel, C.M., Parak, W.J., Gerion, D. & Alivisatos, A.P. Electrophoretic isolation of discrete Au nanocrystal/DNA conjugates. *Nano Lett.* **1**, 32–35 (2001).
49. Sperling, R.A., Pellegrino, T., Li, J.K., Chang, W.H. & Parak, W.J. Electrophoretic separation of nanoparticles with a discrete number of functional groups. *Adv. Funct. Mater.* **16**, 943–948 (2006).
50. Meijering, E., Smal, I. & Danuser, G. Tracking in molecular bioimaging. *IEEE Signal Process. Mag.* **23**, 46–53 (2006).
51. Thompson, R.E., Larson, D.R. & Webb, W.W. Precise nanometer localization analysis for individual fluorescent probes. *Biophys. J.* **82**, 2775–2783 (2002).
52. Cheezum, M.K., Walker, W.F. & Guilford, W.H. Quantitative comparison of algorithms for tracking single fluorescent particles. *Biophys. J.* **81**, 2378–2388 (2001).
53. Bonneau, S., Dahan, M. & Cohen, L.D. Single quantum dot tracking based on perceptual grouping using minimal paths in a spatiotemporal volume. *IEEE Trans. Image Process.* **14**, 1384–1395 (2005).
54. Serge, A., Bertaux, N., Rigneault, H. & Marguet, D. Dynamic multiple-target tracing to probe spatiotemporal cartography of cell membranes. *Nat. Methods* **5**, 687–694 (2008).
55. Jaqaman, K. *et al.* Robust single-particle tracking in live-cell time-lapse sequences. *Nat. Methods* **5**, 695–702 (2008).
With reference 54, this paper describes freely downloadable software for tracking single nanoparticles in image sequences.
56. Qian, H., Sheetz, M.P. & Elson, E.L. Single particle tracking. Analysis of diffusion and flow in two-dimensional systems. *Biophys. J.* **60**, 910–921 (1991).
57. Bouzigues, C. & Dahan, M. Transient directed motions of GABA(A) receptors in growth cones detected by a speed correlation index. *Biophys. J.* **92**, 654–660 (2007).
58. Huet, S. *et al.* Analysis of transient behavior in complex trajectories: application to secretory vesicle dynamics. *Biophys. J.* **91**, 3542–3559 (2006).
59. Meilhac, N., Le Guyader, L., Salome, L. & Destainville, N. Detection of confinement and jumps in single-molecule membrane trajectories. *Phys. Rev. E* **73**, 011915 (2006).
60. Simson, R., Sheets, E.D. & Jacobson, K. Detection of temporary lateral confinement of membrane proteins using single-particle tracking analysis. *Biophys. J.* **69**, 989–993 (1995).
61. Helmuth, J.A., Burckhardt, C.J., Koumoutsakos, P., Greber, U.F. & Sbalzarini, I.F. A novel supervised trajectory segmentation algorithm identifies distinct types of human adenovirus motion in host cells. *J. Struct. Biol.* **159**, 347–358 (2007).
62. Masson, J.B. *et al.* Inferring maps of forces inside cell membrane microdomains. *Phys. Rev. Lett.* **102**, 048103 (2009).
63. Durisic, N. *et al.* Detection and correction of blinking bias in image correlation transport measurements of quantum dot tagged macromolecules. *Biophys. J.* **93**, 1338–1346 (2007).
64. Lidke, D.S. *et al.* Quantum dot ligands provide new insights into erbB/HER receptor-mediated signal transduction. *Nat. Biotechnol.* **22**, 198–203 (2004).
Earliest use of ligand-conjugated QDs for the real-time imaging of EGF-erb/HER signal transduction in live cells.
65. Bouzigues, C., Morel, M., Triller, A. & Dahan, M. Asymmetric redistribution of GABA receptors during GABA gradient sensing by nerve growth cones analyzed by single quantum dot imaging. *Proc. Natl. Acad. Sci. USA* **104**, 11251–11256 (2007).
66. O'Connell, K.M.S., Rolig, A.S., Whitesell, J.D. & Tamkun, M.M. Kv2.1 potassium channels are retained within dynamic cell surface microdomains that are defined by a perimeter fence. *J. Neurosci.* **26**, 9609–9618 (2006).
67. Tamkun, M.M., O'Connell, K.M.S. & Rolig, A.S. A cytoskeletal-based perimeter fence selectively corrals a sub-population of cell surface Kv2.1 channels. *J. Cell Sci.* **120**, 2413–2423 (2007).
68. Bates, I.R. *et al.* Membrane lateral diffusion and capture of CFTR within transient confinement zones. *Biophys. J.* **91**, 1046–1058 (2006).
69. Chen, H., Titushkin, I., Stroscio, M. & Cho, M. Altered membrane dynamics of quantum dot-conjugated integrins during osteogenic

differentiation of human bone marrow derived progenitor cells. *Biophys. J.* **92**, 1399–1408 (2007).
70. Kodippili, G.C. *et al.* Imaging of the diffusion of single band 3 molecules on normal and mutant erythrocytes. *Blood* **113**, 6237–6245 (2009).
71. Crane, J.M., Van Hoek, A.N., Skach, W.R. & Verkman, A.S. Aquaporin-4 dynamics in orthogonal arrays in live cells visualized by quantum dot single particle tracking. *Mol. Biol. Cell* **19**, 3369–3378 (2008).
72. Crane, J.M. & Verkman, A.S. Determinants of aquaporin-4 assembly in orthogonal arrays revealed by live-cell single-molecule fluorescence imaging. *J. Cell Sci.* **122**, 813–821 (2009).
73. Heine, M. *et al.* Surface mobility of postsynaptic AMPARs tunes synaptic transmission. *Science* **320**, 201–205 (2008).
74. Groc, L. *et al.* NMDA receptor surface mobility depends on NR2A–2B subunits. *Proc. Natl. Acad. Sci. USA* **103**, 18769–18774 (2006).
75. Levi, S. *et al.* Homeostatic regulation of synaptic GlyR numbers driven by lateral diffusion. *Neuron* **59**, 261–273 (2008).
76. Mikasova, L., Groc, L., Choquet, D. & Manzoni, O.J. Altered surface trafficking of presynaptic cannabinoid type 1 receptor in and out synaptic terminals parallels receptor desensitization. *Proc. Natl. Acad. Sci. USA* **105**, 18596–18601 (2008).
77. Geng, L., Qian, Y.K., Madhavan, R. & Peng, H.B. Transmembrane mechanisms in the assembly of the postsynaptic apparatus at the neuromuscular junction. *Chem. Biol. Interact.* **175**, 108–112 (2008).
78. Triller, A. & Choquet, D. New concepts in synaptic biology derived from single-molecule imaging. *Neuron* **59**, 359–374 (2008).
79. Charrier, C., Ehrensperger, M.-V., Dahan, M., Levi, S. & Triller, A. Cytoskeleton regulation of glycine receptor number at synapses and diffusion in the plasma membrane. *J. Neurosci.* **26**, 8502–8511 (2006).
80. Groc, L. *et al.* NMDA receptor surface trafficking and synaptic subunit composition are developmentally regulated by the extracellular matrix protein reelin. *J. Neurosci.* **27**, 10165–10175 (2007).
81. Renner, M., Choquet, D. & Triller, A. Control of the postsynaptic membrane viscosity. *J. Neurosci.* **29**, 2926–2937 (2009).
82. Zhang, Q., Cao, Y.Q. & Tsien, R.W. Quantum dots provide an optical signal specific to full collapse fusion of synaptic vesicles. *Proc. Natl. Acad. Sci. USA* **104**, 17843–17848 (2007).
83. Zhang, Q., Li, Y.L. & Tsien, R.W. The dynamic control of kiss-and-run and vesicular reuse probed with single nanoparticles. *Science* **323**, 1448–1453 (2009).
With reference 82, an original use of single QD optical properties and size to address the controversial issues of kiss and run versus full collapse vesicular fusion as a mechanism for presynaptic release in neurons.
84. Cui, B. *et al.* One at a time, live tracking of NGF axonal transport using quantum dots. *Proc. Natl. Acad. Sci. USA* **104**, 13666–13671 (2007).
85. Echarte, M.M., Bruno, L., Arndt-Jovin, D.J., Jovin, T.M. & Pietrasanta, L.I. Quantitative single particle tracking of NGF-receptor complexes: transport is bidirectional but biased by longer retrograde run lengths. *FEBS Lett.* **581**, 2905–2913 (2007).
86. Rajan, S.S., Liu, H.Y. & Vu, T.Q. Ligand-bound quantum dot probes for studying the molecular scale dynamics of receptor endocytic trafficking in live cells. *ACS Nano.* **2**, 1153–1166 (2008).
87. Joo, K.I. *et al.* Site-specific labeling of enveloped viruses with quantum dots for single virus tracking. *ACS Nano.* **2**, 1553–1562 (2008).
88. Courty, S., Luccardini, C., Bellaiche, Y., Cappello, G. & Dahan, M. Tracking individual kinesin motors in living cells using single quantum-dot imaging. *Nano Lett.* **6**, 1491–1495 (2006).
First report of QD use for intracellular tracking, with a study of individual kinesin motor movements in the cytoplasm of live cells.
89. Pierobon, P. *et al.* Velocity, processivity, and individual steps of single myosin V molecules in live cells. *Biophys. J.* **96**, 4268–4275 (2009).
90. Nelson, S.R., Ali, M.Y., Trybus, K.M. & Warshaw, D.M. Random walk of processive, quantum dot-labeled myosin Va molecules within the actin cortex of COS-7 cells. *Biophys. J.* **97**, 509–518 (2009).
91. Keren, K., Yam, P.T., Kinkhabwala, A., Mogilner, A. & Theriot, J.A. Intracellular fluid flow in rapidly moving cells. *Nat. Cell Biol.* **11**, 1219–U137 (2009).
92. Ishihama, Y. & Funatsu, T. Single molecule tracking of quantum dot-labeled mRNAs in a cell nucleus. *Biochem. Biophys. Res. Commun.* **381**, 33–38 (2009).
93. Wells, N.P. *et al.* Going beyond 2D: following membrane diffusion and topography in the IgE-Fc[epsilon]RI system using 3-dimensional tracking microscopy. *Proc. SPIE* **7185**, 71850Z-1–71850Z-13 (2009).
94. Holtzer, L., Meckel, T. & Schmidt, T. Nanometric three-dimensional tracking of individual quantum dots in cells. *Appl. Phys. Lett.* **90**, 053902-1–053902-3 (2007).
95. Ram, S., Prabhat, P., Chao, J., Ward, E.S. & Ober, R.J. High accuracy 3D quantum dot tracking with multifocal plane microscopy for the study of fast intracellular dynamics in live cells. *Biophys. J.* **95**, 6025–6043 (2008).
96. Thompson, M.A., Lew, M.D., Badieirostami, M. & Moerner, W.E. Localizing and tracking single nanoscale emitters in three dimensions with high spatiotemporal resolution using a double-helix point spread function. *Nano Lett.* **10**, 211–218 (2010).
97. Choi, H.S. *et al.* Renal clearance of quantum dots. *Nat. Biotechnol.* **25**, 1165–1170 (2007).
98. Smith, A.M. & Nie, S. Minimizing the hydrodynamic size of quantum dots with multifunctional multidentate polymer ligands. *J. Am. Chem. Soc.* **130**, 11278–11279 (2008).
99. Xie, R., Battaglia, D. & Peng, X. Colloidal InP nanocrystals as efficient emitters covering blue to near-infrared. *J. Am. Chem. Soc.* **129**, 15432–15433 (2007).
100. Zimmer, J.P. *et al.* Size series of small indium arsenide-zinc selenide core-shell nanocrystals and their application to *in vivo* imaging. *J. Am. Chem. Soc.* **128**, 2526–2527 (2006).
101. Hohng, S. & Ha, T. Near-complete suppression of quantum dot blinking in ambient conditions. *J. Am. Chem. Soc.* **126**, 1324–1325 (2004).
102. Chen, Y. *et al.* Giant multishell CdSe nanocrystal quantum dots with suppressed blinking. *J. Am. Chem. Soc.* **130**, 5026–5027 (2008).
103. Mahler, B. *et al.* Towards non-blinking colloidal quantum dots. *Nat. Mater.* **7**, 659–664 (2008).
104. Wang, X. *et al.* Non-blinking semiconductor nanocrystals. *Nature* **459**, 686–689 (2009).
105. Misteli, T. The concept of self-organization in cellular architecture. *J. Cell Biol.* **155**, 181–185 (2001).
106. Huang, B., Bates, M. & Zhuang, X. Super-resolution fluorescence microscopy. *Annu. Rev. Biochem.* **78**, 993–1016 (2009).
107. Ulbrich, M.H. & Isacoff, E.Y. Subunit counting in membrane-bound proteins. *Nat. Methods* **4**, 319–321 (2007).
108. Delehanty, J., Mattoussi, H. & Medintz, I. Delivering quantum dots into cells: strategies, progress and remaining issues. *Anal. Bioanal. Chem.* **393**, 1091–1105 (2009).
109. Jaiswal, J.K., Mattoussi, H., Mauro, J.M. & Simon, S.M. Long-term multiple color imaging of live cells using quantum dot bioconjugates. *Nat. Biotechnol.* **21**, 47–51 (2003).
110. Derfus, A.M., Chan, W.C.W. & Bhatia, S.N. Intracellular delivery of quantum dots for live cell labeling and organelle tracking. *Adv. Mater.* **16**, 961–966 (2004).
111. Delehanty, J.B. *et al.* Self-assembled quantum dot-peptide bioconjugates for selective intracellular delivery. *Bioconjug. Chem.* **17**, 920–927 (2006).
112. Ruan, G., Agrawal, A., Marcus, A.I. & Nie, S. Imaging and tracking of Tat peptide-conjugated quantum dots in living cells: new insights into nanoparticle uptake, intracellular transport, and vesicle shedding. *J. Am. Chem. Soc.* **129**, 14759–14766 (2007).
113. Chan, W.C.W. & Nie, S.M. Quantum dot bioconjugates for ultrasensitive nonisotopic detection. *Science* **281**, 2016–2018 (1998).
114. Tekle, C., v Deurs, B., Sandvig, K. & Iversen, T.-G. Cellular trafficking of quantum dot-ligand bioconjugates and their induction of changes in normal routing of unconjugated ligands. *Nano Lett.* **8**, 1858–1865 (2008).
115. Yoo, J., Kambara, T., Gonda, K. & Higuchi, H. Intracellular imaging of targeted proteins labeled with quantum dots. *Exp. Cell Res.* **314**, 3563–3569 (2008).
116. Kim, B.Y.S. *et al.* Biodegradable quantum dot nanocomposites enable live cell labeling and imaging of cytoplasmic targets. *Nano Lett.* **8**, 3887–3892 (2008).
117. Duan, H. & Nie, S. Cell-penetrating quantum dots based on multivalent and endosome-disrupting surface coatings. *J. Am. Chem. Soc.* **129**, 3333–3338 (2007).
118. Qi, L. & Gao, X. Quantum dot-amphipol nanocomplex for intracellular delivery and real-time imaging of siRNA. *ACS Nano* **2**, 1403–1410 (2008).
119. Jablonski, A.E., Humphries, W.H. & Payne, C.K. Pyrenebutyrate-mediated delivery of quantum dots across the plasma membrane of living cells. *J. Phys. Chem. B* **113**, 405–408 (2009).
120. Chen, X., Kis, A., Zettl, A. & Bertozzi, C.R. A cell nanoinjector based on carbon nanotubes. *Proc. Natl. Acad. Sci. USA* **104**, 8218–8222 (2007).
121. Park, S., Kim, Y.-S., Kim, W.B. & Jon, S. Carbon nanosyringe array as a platform for intracellular delivery. *Nano Lett.* **9**, 1325–1329 (2009).